Measurements of Velocity Profiles and Static Pressure Recovery in a Wide-Angled Diffuser

K. Kibicho[1] and A.T. Sayers[2]

Received 2 April 2008, in revised form 4 July 2008 and accepted 7 July 2008

The difficulties in understanding severely asymmetrical flows in wide-angled diffusers are associated with a lack of sufficient experimental data and accurate flow prediction methods. To address this inadequacy, experimental velocity profiles and static pressure recovery data, which were obtained in a wide-angled diffuser of divergence angle of 30°, are presented in this paper. The measurements were carried out at Reynolds numbers between 1.07×10^5 and 2.14×10^5 based on inlet hydraulic diameter and centreline velocity. Due to the adverse pressure gradient along the diffuser walls in wide-angled diffusers, the attached flow separates from one diverging wall and remains attached permanently to the other wall. Tests performed to determine the wall to which the flow remained attached led to the conclusion that the wall of preference was totally random. Results showed that regardless of the wall to which the flow was attached, both the velocity and pressure fields were replicated with discrepancies below 2 %. The experimental uncertainties were also below 2 %. Within these uncertainties, a reliable data bank contribution for flows in a 30° diffuser has been made.

Additional Keywords: Two-dimensional, stall, separated flows, subsonic flows, diffuser flow regimes

Nomenclature

Based on figure 1

Roman

- AR area ratio (W_2/W_1)
- AS aspect ratio (b/W_1)
- C_p coefficient of pressure recovery in the two-dimensional diffuser
- $f(\psi)$ yaw meter calibration parameter
- L length along the wall of the diffuser measured from the diffuser inlet, [m]
- L/W_1 length to width ratio
- P_D dynamic pressure ($0.5\rho u^2$) [N/m^2]
- P_S static pressure [N/m^2]
- Q_p yaw meter dynamic pressure calibration parameter
- S_p yaw meter total pressure calibration parameter
- u,v velocity measured in x and y directions respectively [m/s]
- x distance measured from diffuser inlet along the x axis [m]
- W_1 width of diffuser at entry [m]
- y, z distances measured about x axis in y and z directions respectively [m]

Greek

- θ diffuser divergence half angle [degrees]
- ρ density of air [kg/m^3]
- ψ flow direction measured by the yaw meter [degrees]

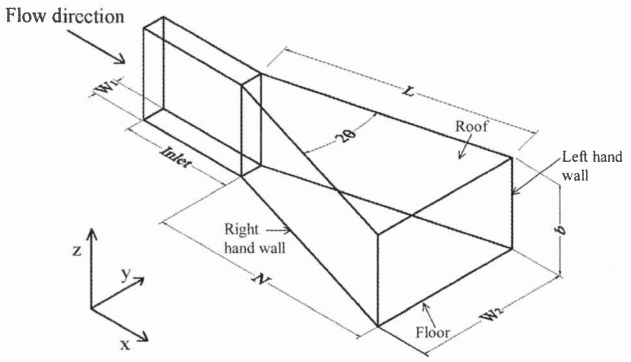

Figure 1: Two-dimensional diffuser notation and frame of reference

1. Introduction

Diffusers are found in many fluid-flow systems, such as turbo machines, flow meters, noise suppressors, air-conditioning ducting, wind tunnels etc, and are usually designed to operate in the unstalled condition. However, to meet some design constraints such as the overall size of the fluid flow systems, wide angled diffusers, which undergo stall, are often tolerated, especially when the area ratios are specified. For small diffuser divergence angles of less than 7°, there is no appreciable reversed flow. But as the divergence angle is increased, the adverse pressure gradient along the diffuser walls causes flow separation with an appreciable back flow in the diffuser. This type of flow is highly unsteady. However, at large divergence angles, the stall becomes fully developed and steady and attaches itself permanently to one wall. The diffuser investigated in this paper falls under this category. At very large divergence angles, the flow separates from both walls in what is known as a jet flow. These flow regimes are described in detail by Kline et al.[1] and Reneau et al.[2] and are shown in figure 2. Whenever stall in diffuser flows occurs, regions of stalled flow block the normal flow causing poor pressure recovery and severe asymmetry of the flow. It has been known for many years that the maximum pressure recovery in a diffuser is attained when there is appreciable stall in the diffuser, and occurs when the total included angle is between 7-10°.

The flow-field and performance of a diffuser is affected by many parameters. Primary among them are; Reynolds number, level of turbulence at the diffuser inlet, and diffuser geometry. For a given inlet geometry, and when the flow Reynolds number

1 Jomo Kenyata University of Agricultural Technology, Kenya.
2 MSAIMech E, Department of Mechanical Engineering, University of Cape Town, Rondebosch, 7700, South Africa
E-mail: Anthony.Sayers@uct.ac.za

is high, the coefficient of pressure recovery and the flow regimes, shown in figure 2, are not significantly affected by a variation in the Reynolds number. However, the diffuser performance is improved by an increase in the inlet free-stream level of turbulence. The effects of these parameters on performance have been reported by Waitman et al.[3], Carlson et al.[4], Johnston and Powars[5], and Wolf and Johnston[6]. An understanding of the relationships between these parameters and their effects on the diffuser performance leads to a rational basis for diffuser design and the use of experimental data to develop and validate numerical codes.

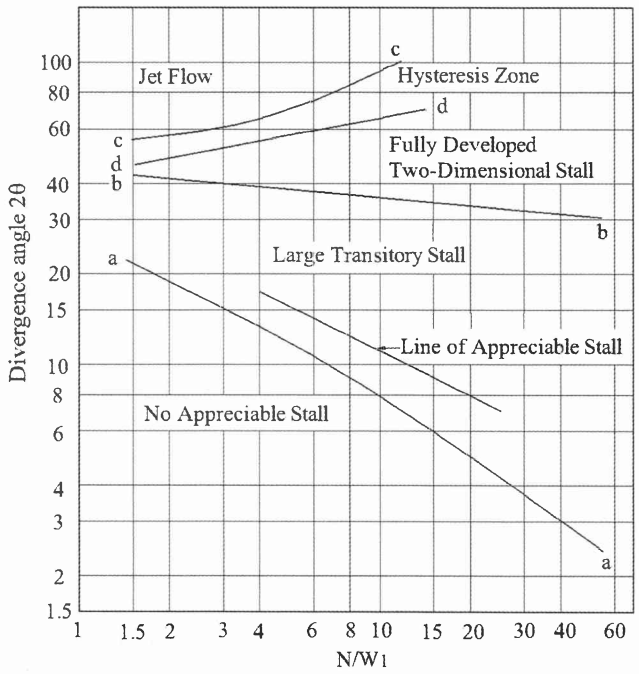

Figure 2: Flow regimes in two-dimensional diffusers

Buice and Eaton[7] have carried out very reliable experimental measurements on velocity and static pressure profiles, and pressure recovery data, for narrow asymmetric diffusers. However, little experimental data for wide-angled diffuser flows are available, while of the available literature, only wall static pressure recovery data is provided. Besides that, there are no successful theoretical methods that exist for diffuser flows which are stalled, hence careful and systematic data on flows in wide angled diffusers are required to solve this long standing, but still important diffuser flow problem. It is against this background that the measurements described in this paper were obtained.

2. Experimental Apparatus and Instrumentation

The experimental apparatus is shown in figure 3. Air was delivered by a radial flow fan into a 1.9 m long, rectangular-circular transition duct, which was connected to a 600 mm inner diameter, 3.7 m long circular duct. A 1 m long circular-rectangular transition duct transferred the air to a 400 mm × 100 mm × 1 m long straight inlet duct before its entry into the diffuser proper. After flowing through the diffuser the air was discharged back into the atmosphere.

The diffuser was of plane wall with the roof and floor walls running parallel to each other. The overall error in parallelism for the roof and floor was ±0.25 mm. Further, the distances between the left and right walls at both entry to and exit from the diffuser were measured and the error in the divergence angle based on these measurements was found to be ±0.24°. All the plates for the straight inlet section and diffuser were machined from 10 mm thick transparent thermoplastic resin (Perspex) and all sections of the duct were bolted through flanges.

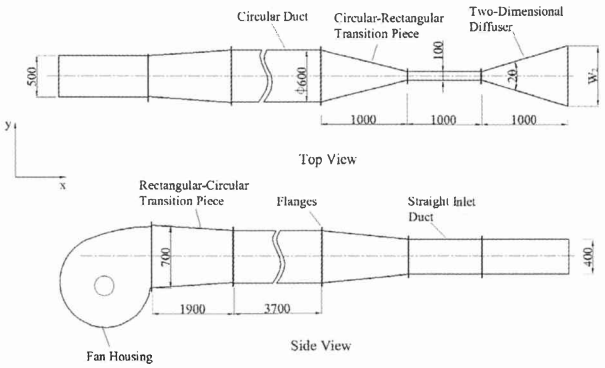

Figure 3: Experimental apparatus

Before the diffuser was bolted to the straight inlet duct, measurements showed that the flow at the exit of this duct was symmetrical about the x axis in both the y and z directions. However, as Wolf and Johnston[6], and, Kaiser and McDonald[8] have shown, once the diffuser is connected to the straight duct, the presence of stall in the diffuser distort the velocity profile at the exit of the straight duct. It was desired to measure the reference flow parameters at a location where the flow was symmetrical about the x-axis in both the y and z directions, and hence an arbitrary upstream location in the straight duct, x/W_1=–2.35, where these flow conditions were met, was chosen as a suitable flow reference location.

At the diffuser entry, the edges of the entry duct side plate and diffuser entry side plate were machined at appropriate angles to form the required divergence angle on assembly. These side plates were joined using chloroform, and the sharp edges at the entry corners smoothened very carefully by use of a fine file and sand paper to form the diffuser corner assembly whose details are shown in figure 4. The diffuser side plate that was joined to the corner plate was 903 mm long. To straighten the flow, wire mesh screens of 0.9 mm wire thickness, 3.3 mm square eye and 6 holes per square centimetre were installed at the rectangular-circular transition piece exit, circular duct-transition piece interface and transition piece-entry duct interface.

At the reference point, eight static pressure holes of 1.8 mm diameter, were drilled, two on each side of the duct. Due to the manufacturing difficulties of drilling the 1.8 mm holes at the exact diffuser entry, a similar set of eight holes were drilled at a location 2 mm upstream of the diffuser entry. This is the point at which the entry static pressure, P_1, was measured. The static pressures at the reference location and at the diffuser entry were averaged by connecting the eight tubes, to a common ring tube through 1.5 mm flexible vinyl tubing, at each of the two locations. The output of the common ring tube at the reference point was used as the reference pressure, P_{ref}, in all the experiments,

while the output of the ring tube at the diffuser entry was the inlet static pressure, P_1. The static pressure P_1 was used as the reference inlet pressure against which pressure recovery values at points along the sidewall, $P_x - P_1$, were evaluated.

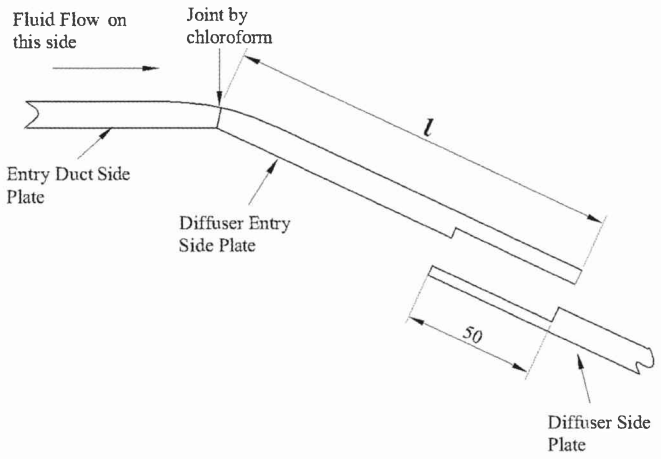

Figure 4: The diffuser corner assembly details

A port for the insertion of a Pitot tube from the side was provided at the flow reference point for measurement of the total pressure, and hence the average entry axial velocity, U_1 was established.

On each side plate of the inlet duct-diffuser assembly, 60 static pressure holes, and hence a total of 120 static pressure holes for both sides, were drilled. Attention was paid to the locations near the entry of the diffuser where very high pressure gradients due to separation and a sudden change of flow geometry were expected. In this region, the static pressure holes were spaced at 5 mm intervals. This spacing increased progressively to 10, 20 and 50 mm in the downstream direction.

The roof of the diffuser was constructed from six 150 mm wide strips and two strips of widths 15 mm and 85 mm installed as the first and last strip at the entry and exit of the diffuser respectively. All the strips were made from 10 mm Perspex and were reinforced with 25 mm aluminium square tubes. A 150 mm wide Perspex probing strip was used to move a 3-tube yaw meter in the y direction for measuring the velocity profiles across the diffuser test section. To ensure that during probing, the diffuser roof remained covered even at the widest position, this strip was 2 m long, 10 mm thick and was also reinforced with a 25 mm aluminium square tube. All the 150 mm wide roof strips were removed in turn and replaced with the probing strip. Velocity profiles were then measured at 150 mm intervals in the x direction along the axial length of the diffuser.

All the pressures were measured using a 0-625 Pa full range reluctance differential pressure transducer whose voltage signals were conditioned and calibrated at manufacture to give a linearized 0-5Vdc output at an accuracy of ±1.5 % full scale. The low-pressure port of the transducer was connected to the averaged static pressure tapping at the flow reference point, while the high-pressure port was connected to the output of a Scanivalve® pressure scanner. Data was sampled at a frequency of 100 Hz.

A Scanivalve® pressure scanner with 48 pressure ports was used to scan the static pressures on the diffuser sidewalls, and the total pressure at the reference point. The static pressure tubes were connected to ports 1-47 of the scanner, which meant that three runs were required, in order to take measurement at all the 120 static pressure ports on the diffuser side walls for any given inlet flow Reynolds number. The total pressure Pitot tube was connected to port 48 of the scanner, and hence the dynamic pressure, P_D for any run could be established. The dynamic pressure determined from the total and static pressures measured at the flow reference point for each run was then used to normalize all the static pressures measured for that run. Therefore, any variations in the coefficient of pressure recovery that could result from changes in flow and atmospheric conditions were minimized. The coefficients of pressure recovery, C_p, were evaluated according to the definition given in equation 1.

$$C_p = \frac{P_x - P_1}{\frac{1}{2}\rho U_1^2} \tag{1}$$

Probing was done using a 3-tube yaw meter. The probe was calibrated against a hot-wire anemometer in a low-turbulence intensity (0.4 % turbulence intensity) wind tunnel flow field. The reference probe null-direction was selected as the direction of the centreline of the probe tip in line with the main flow direction when the pressures recorded from the off-centre tubes were equal to each other. At this reference direction, $\psi = 0$. The pressure measured at the central tube of the probe at this position was the total (stagnation) pressure of the flow, P_t. Non-dimensional calibration parameters were calculated in terms of pressures and resultant flow velocity, q, similar to those specified by Yajnik and Gupta[9], Gundogdu and Carpinlioglu[10] and Rhagava et al.[11] and given in equations 2 to 4.

$$f(\psi) = \frac{P_l - P_r}{P_c - P_m} \tag{2}$$

$$Q_p = \frac{P_c - P_m}{\frac{1}{2}\rho q^2} \tag{3}$$

$$S_p = \frac{P_t - P_c}{P_c - P_m} \tag{4}$$

where P_l and P_r are the pressures sensed by the off-centre tubes, $P_m = (P_l + P_r)/2$, is the mean pressure for the off-centre pressures, P_c is the pressure measured by the central tube, and P_t is the local total pressure that would be measured by the probe if it were at the null-position. These functions can be established directly and are known to be independent of Reynolds number. Thus, once established at one Reynolds number, they can be applied to a range of Reynolds numbers. Calibration of the probe was done at 15 m/s. The resulting chart for $f(\psi)$ is shown in figure 5. For the large number of measurement points, reading the

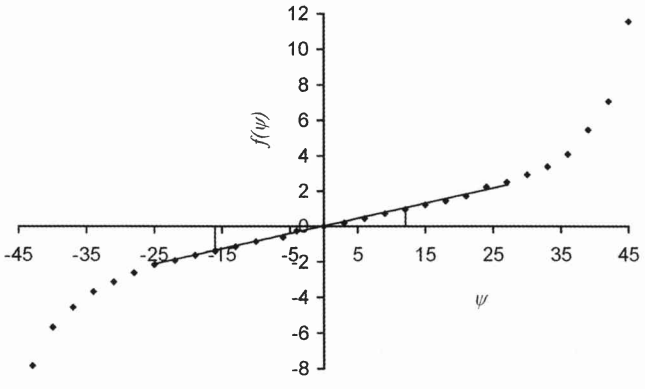

Figure 5: Yaw angle calibration parameter $f(\Psi)$ for $-45° < \Psi < 45°$

calibration parameters from the charts proved to be tedious. Consequently, the linear portions of the calibration charts were established, and polynomial descriptions of these portions developed so that the analysis could be simplified by processing the parameters using a personal computer. The linear portion of the $f(\psi)$ versus ψ chart was found to be between $-1.4<f(\psi)<1.26$ which corresponded to $-16°<\psi<14°$ and was described by equation 5.

$$f(\psi) = 0.0295 + 0.089 \cdot \psi \tag{5}$$

Within this region, the dynamic pressure, Q_p, and total pressure, S_P calibration parameters both produced a one on one relationship with ψ and were curve fitted using sixth order polynomials given in equations 6 and 7.

$$Q_p = 0.6544 + (26\psi - \psi^2) \times 10^{-4} - (3\psi^3 - \psi^4) \times 10^{-6} - (7\psi^5 + 3\psi^6) \times 10^{-9} \tag{6}$$

$$S_p = 0.0079 - (5\psi - 3\psi^2) \times 10^{-4} - (\psi^3 + 5\psi^4) \times 10^{-6} + (20\psi^5 + 4\psi^6) \times 10^{-9} \tag{7}$$

To avoid a singularity in equations 2 and 4, when $(P_c - P_m)$ becomes zero, it was ensured that $(P_c - P_m)$ remained positive by rotating the probe in the appropriate direction and hence changing the readings of P_l and P_r. This condition was monitored through the data acquisition software. Negative values of $(P_c - P_m)$, and hence Q_p, would describe complex imaginary values of the velocity based on equation 3. Values of $f(\psi)$ were also monitored real time so that whenever they were out of range $(-1.4<f(\psi)<1.26)$, they would be adjusted accordingly by rotating the probe in the appropriate direction thereby changing the values of P_l and P_r. The value of ψ is then established from equation 5. Thereafter, the flow direction and velocity were established relative to the adjusted probe direction. Finally, the calculated flow direction was transformed so that it was referenced to the geometric null-probe direction. At a given location, equations 2 and 5 were used to evaluate the yaw calibration parameter, $f(\psi)$, and the yaw angle, ψ respectively. The dynamic pressure calibration parameter, Q_p, and the local dynamic pressure were calculated from equations 3 and 6. Finally, the total pressure calibration parameter, S_P, and total pressure, and, hence static pressure were established from equations 4 and 7. The velocity components u and v with respect to the x and y-directions of the pressure probe, respectively, were calculated according to equations 8.

$$u = q\cos\psi \qquad v = q\sin\psi \tag{8}$$

Results obtained by use of these polynomials were tested at several locations within the diffuser test section against the null-reading technique. The average error in measuring the flow angle was 0.81°. The rms error in velocity measurement was 1.37 %.

All the voltage signals obtained from the reluctance transducer and the hot wire anemometer were digitized through a plug-in 32-bit PCI data acquisition board (DAQ). The board had an internal IDC40 connector for digital I/O, through which, the Scanivalve® controller and an odd-even decoder were interfaced to the computer. Data acquisition software was developed using the National Instruments' LabVIEW programme.

3. Results and Discussion

The inlet flow conditions of a diffuser as characterized by the blockage factor and level of turbulence influence the diffuser performance. The inlet axial velocity profiles were measured, first without the diffuser and then repeated with the diffuser connected to the inlet duct. Introduction of the diffuser introduced serious asymmetry of the inlet flow. The asymmetry of the flow, λ, was evaluated as the overall percentage discrepancy of axial velocities u_i, measured at corresponding points to the right and left of the x-axis. By attaching the diffuser to the straight inlet duct, the asymmetry of the flow at the diffuser entry was measured to be less than 5 % for all the Reynolds numbers tested in this study. The asymmetry of the flow caused the corresponding static pressures on the opposite side walls at the inlet to be different. This situation presented a problem in the interpretation of reference inlet conditions both for the velocity and static pressure data, since each flow condition produced different profiles. Consequently, it was found necessary to reference the inlet flow conditions to a location where the flow was reasonably uniform. Such a point was found to be at an arbitrarily chosen upstream location of x/W_1=–2.35. At this inlet reference location, the axial velocity profiles were again measured, with and without the diffuser. At this location the asymmetry reduced to less than 0.20 % in both y and z directions.

All the measurements in the inlet duct were carried out using a single hot-wire anemometer. The blockage factors were approximately 0.014 and hence the pressure recovery data can be compared with the data of Reneau et al.[2], which is available for $B = 0.015$.

It still remains unclear why stall in the two-dimensional fully stalled regime in diffusers occurs on a particular wall. As described earlier, great care was taken to manufacture a highly symmetrical diffuser. Tests to rule out the possibility of a bias towards the flow attaching to a particular wall whenever the fan was switched on were carried out. In this regard, before any measurements were taken, a start-stop check was done whereby the fan was started, the wall to which the flow was attached noted, the fan switched off and started again and the process repeated. An intermittency parameter γ_s, was then defined as a ratio of the number of times the flow remained attached to a given wall to the total number of start-stop cycles. After 50 cycles γ_s was found to be 0.45 and 0.55 for the right hand and left hand stalls, respectively. While it might be difficult to manufacture a perfectly symmetrical diffuser, these results imply that there is more to the stall bias than just the small manufacturing imperfections that might be present in the diffuser. It was however, possible to force the flow to attach to the other wall by partially blocking the flow at the inlet with a piece of Perspex, and directing it to the desired wall. Once 'switched' to the other wall, the flow remained attached to that wall.

Flows in wide angled diffusers are inherently unsteady. In order to reduce the effect of the unsteadiness in the experimental results, the pressure transducer differential voltages were averaged over long durations. The optimal averaging duration corresponded to the period beyond which the velocity and static pressure readings at a few selected points remained constant for a given inlet flow velocity. This optimal averaging time was kept constant for the rest of the measurements and it was only then that the repeatability tests to determine the overall experimental uncertainties were performed.

Due to the large number of data points obtained especially when measuring the velocity profiles, it was found adequate to take readings at each point three times and then average their discrepancies for all the data points. In any case, the statement of overall uncertainties is all that is required. The results were repeatable to within less than 1.65 % and 0.4 % for static pressure and velocity profiles respectively.

As has already been discussed, the wall to which the flow attached was quite random. With this in mind, it was important to confirm that both the pressure and velocity fields were independent of the wall to which flow was attached. To verify this requirement, the flow field was measured with the flow firstly attached to the left wall and secondly with the flow attached to the right wall, as can be seen in figure 6.

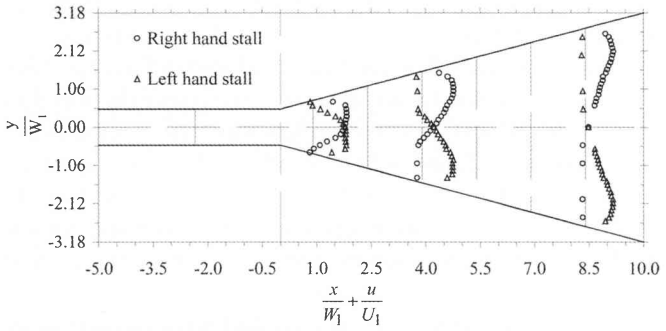

Figure 6: Replication of velocity profiles

Lastly, static pressures were measured on the wall to which the flow was attached (unstalled wall). Pressure recovery data for corresponding static pressure holes on the two walls is shown in figure 7. The velocity profiles were replicated with a discrepancy of 0.6 % while the wall static pressure was within 2 %.

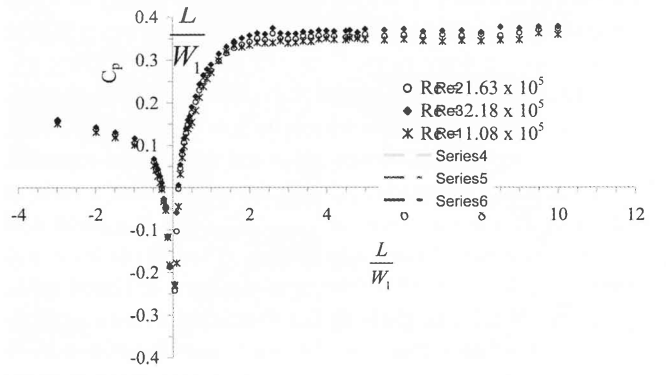

Figure 7: Replication of C_p

The static pressure field showed more sensitivity to replication than the velocity profiles. However, since the replication discrepancies are of the same order of magnitude as the repeatability, they can be viewed to be a result of the flow unsteadiness and the small imperfections in the diffuser symmetry. However, since the data acquisition system was placed on the left side of the diffuser, the flow was always manually 'switched' to the left wall in instances when it attached to the right wall.

Although it is reported in the literature (for example Reneau et al.[2]) that variation of Reynolds number does not influence the pressure recovery data, the indications obtained while performing the repeatability and replication tests, was that Reynolds number indeed has a significant influence on the flow field. It was therefore decided to perform tests to evaluate the influence of Reynolds number on both the static pressure and velocity field. The inlet velocity was set at 10 m/s, 15 m/s and 20 m/s corresponding to Reynolds numbers 1.08×10^5, 1.63×10^5, 2.18×10^5, respectively. Preliminary tests showed that higher velocities produced undesirable vibration of the diffuser. Figures 8 and 9 show the influence of the Reynolds number on the wall static pressure recovery and velocity profiles respectively.

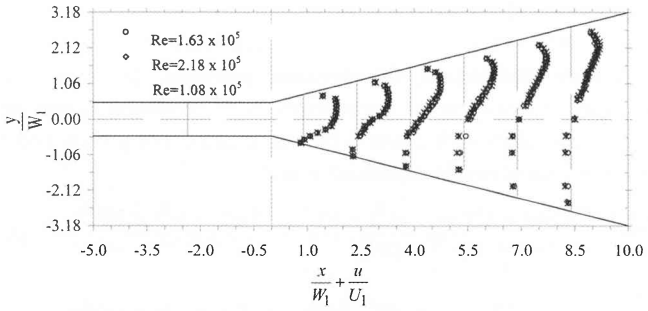

Figure 8: Influence of Re on velocity profiles

It can be observed from figure 9 that near the diffuser inlet the influence of Reynolds number on static pressure recovery is significant. The sensitivity of C_p values to Reynolds number changes can be attributed to the three-dimensional nature of the flow expected in this region and to the fact that it is in this region that the highest adverse pressure gradients are experienced, rendering the flow here very unstable. Attempts to use the yaw meter to measure the velocity profiles in this region resulted in data whose repeatability was above 15 %. However, velocity profiles measured at the first strip (located 90 mm downstream

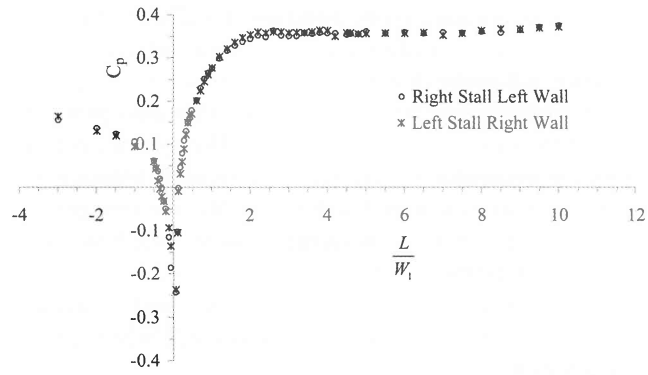

Figure 9: Influence of Re on C_p

of the diffuser inlet) indicated very little influence (of the order of 1 %) on the profiles due to Reynolds numbers. To get an indication of the influence of Reynolds number and yet include results from this very unstable region, some out-of-range discrepancy results were statistically rejected using Chauvenet's data rejection criteria (Taylor[12]). With this treatment of data, the results show that by changing the velocity from 10 m/s to 20 m/s, the static pressure recovery increased by 8.31 %. A similar data treatment approach adopted for the velocity profiles showed that the increase of the normalized velocities, for a similar increase in Reynolds number, was 1.37 %. Evidently, the static pressure was influenced by the Reynolds number at values that are outside the uncertainties of this study. It might be of interest

in future to carry out a study that can relate, Reynolds number to diffuser geometry. Results from the limited number of flow cases in this study cannot be considered adequate to provide a reasonable correlation. Bearing this in mind and in order to focus on the primary objectives of this study, it was decided that from this point onwards, the Reynolds number be held constant at 1.63×10^5 corresponding to an inlet duct velocity of 15 m/s.

The primary assumption made in this study is that the flow is two-dimensional. In fact, it is only due to this assumption that the three-tube yaw meter was used to measure the velocity vectors. Since for the diffuser under investigation, the roof and the floor walls ran parallel to each other, it was rational to assume that the boundary layer growth rates from the floor and roof walls were the same and merged at the mid-plane. Therefore, measuring the flow in the mid-plane was adequately representative of a two-dimensional flow. Traditionally, proof of two-dimensionality of a flow is carried out by measuring axial velocity profiles at two different planes, one below the mid-plane, and another above the mid-plane. Thus, for a given location within the diffuser, axial velocity profiles were measured in three planes, namely; upper, mid and lower planes. Consequently, the two-dimensionality of the flow was verified using this procedure, with the velocity profiles being measured at three locations downstream of the diffuser inlet located at x/W_1= 0.9, 3.9 and 8.4. Results from such measurements are shown in figure 10.

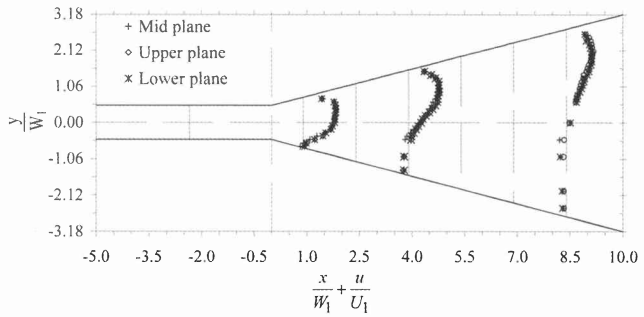

Figure 10: Two-dimensionality test

For symmetrical boundary layer growth rates between roof and floor walls, the velocity profiles in the upper and lower planes, must be the same. With the mid-plane held as the datum, the largest deviation for both the upper and lower planes was 0.1 %. This meant that the two-dimensionality was well within the uncertainties of the experimental data in this study. However, the lower plane consistently gave higher discrepancies, in line with what Kline[13] observed about the stall starting at a localized position on the lower corners of the diffuser before spreading to the rest of the diffuser. Flow visualization using woollen tufts was performed in order to observe the steadiness and two-dimensionality of the flow. The woollen tufts were attached to the sidewalls of the diffuser at several locations. Apart from the tufts that were next to the roof and floor, and which displayed slight fluctuations of movement, all the other tufts faced the downstream direction steadily and ran almost parallel to each other.

4. Conclusions

In this study, experimental investigations of separated flows in fully stalled wide-angled diffuser have been carried out. Due to the adverse pressure gradient along the diffuser walls, flow separated from one diverging wall and became attached to the other wall, thus forming a region of steady stall within the diffuser. It was not possible to determine in advance, the wall to which the flow would attach. Tests to determine the wall to which the flow remains attached led to the conclusion that the wall of preference was totally random and was probably caused by a slight upstream disturbance that was impossible to detect. However, it was possible to 'switch' the flow from one wall to the other by introducing an inlet disturbance. It was found that once 'switched' to a wall, the flow remained attached to that wall permanently. Experimental results showed that regardless of the wall to which the flow was attached, both the velocity and pressure flow-fields were replicated with discrepancies below 2 %. Although current literature states that for a given geometry, the Reynolds number has little influence on the static pressure recovery, it was found in this study that by increasing the velocity from 10 m/s to 20 m/s, the static pressure recovery increased by 8.31 %. The limited range of Reynolds numbers investigated in this study could not allow a rational correlation between the Reynolds number and the C_p profiles. This range was limited by the physical constraints imposed by the wind tunnel and fan speed. For instance, a change of velocity from 10 m/s to 80 m/s would not change the Reynolds number by even one order of magnitude. The experimental uncertainties in this research were approximately 2 %. Within these uncertainties a reliable data bank contribution has been provided for a 30° diffuser. The parameters in the data bank include the wall static pressure recovery data, axial and lateral velocity profiles and static pressure profiles.

References

1. *Kline SJ, Abbort DE and Fox RW*, Optimum design of straight-walled diffusers, *Transactions of the ASME, Journal of Basic Engineering*, 1959, 81, 321-331.

2. *Reneau R, Johnston JP and Kline SJ*, Performance and design of straight, two-dimensional diffusers, *Transactions of the ASME, Journal of Basic Engineering*, 1967, 89(1), 141-150.

3. *Waitman BA, Reneau LR and Kline SJ*, Effects of inlet conditions on performance of two-dimensional diffusers, *Transactions of the ASME, Journal of Basic Engineering*, 1961, 83(3), 349-360.

4. *Carlson JJ, Johnston JP and Sagi CJ*, Effects of wall shape on flow regimes and performance in straight, two-dimensional diffusers, *Transactions of the ASME, Journal of Basic Engineering*, 1967, 89(1), 151-160.

5. *Johnston JP and Powars CA*, Some effects of inlet blockage and aspect ratio on diffuser performance, *Transactions of the ASME, Journal of Basic Engineering*, 1969, 91, 551-553.

6. *Wolf S, and Johnston JP*, Effects of non-uniform inlet velocity profiles on flow regimes and performance in two-dimensional diffusers, *Transactions of the ASME, Journal of Basic Engineering*, 1969, 91(3), 462-474.

7. *Buice CU and Eaton JK*, Experimental Investigation of Flow Through an Asymmetric Plane Diffuser, 1997, Report No. TSD 107: Center for Turbulence Research, Stanford University.

8. *Kaiser KF and McDonald AT*, Effect of wake-type non-uniform inlet velocity profiles on first appreciable stall in plane-wall diffusers, *Transactions of the ASME, Journal of Fluids Engineering*, 1980, 102(3), 283-289.

9. *Yajnik KS and Gupta RP*, A new probe for measurement of velocity and flow direction in separated flows, *Journal of Physics, Series E, Science Instrumentation*, 1973, 6, 82-86.
10. *Gundogdu MY and Carpinlioglu MO*, A multi-tube pressure probe calibration method for measurements of mean flow parameters in swirling flows, *Flow Measurement and Instrumentation*, 1998, 9, 243-248.
11. *Rhagava AK, Kumar KL, Malhotra RC and Agrawal DP*, A probe for the measurement of velocity field, *Transactions of the ASME, Journal of Fluids Engineering*, 1979, 11(1), 143-146.
12. *Taylor RJ*, An Introduction to Error Analysis, 2 ed., Sausalito, California, USA: University Science Books, 1982.
13. Kline SJ, On the nature of stall, *Transactions of the ASME, Journal of Basic Engineering*, 1959, 81, 305-321.